

# Femtosecond pulsed laser deposition of thin films upon direct and inverse transfer of ablated particles of foam graphite in the nitrogen atmosphere

V.M. Gordienko, V.A. D'yakov, Yu.Ya. Kuzyakov, I.A. Makarov, E.V. Rakov, M.A. Timofeev

**Abstract.** The comparative study of the preparation of carbon films by the methods of direct and inverse femtosecond laser deposition in the nitrogen atmosphere is performed for the first time. It is found that the surface of the film prepared by the method of inverse laser deposition does not virtually contain microparticles, whereas the surface of the directly deposited film is covered by many microparticles. The dependence of the film-surface roughness parameter on the radius (the distance to the centre of the deposition region) is measured. It is shown that the surface roughness of the film on the inverse collector is smaller than that on the direct collector. The ablation rates of foam graphite and volumes of the material ejected and deposited per laser shot are determined.

**Keywords:** femtosecond ablation, foam graphite, pulsed laser deposition.

## 1. Introduction

In recent years the deposition of thin-film carbon coatings by the femtosecond laser ablation of graphite in the atmosphere of various gases attracts great interest [1–5]. The traditional method is based on the direct deposition of films by using nanosecond laser pulses, when ablation products from the expanding plasma plume are collected on a collector located at some distance from a target [6]. The use of buffer gases provides the efficient control of the physical properties of films (surface morphology, electro-optical parameters, etc.) and their chemical properties (by using chemically active gases).

The physical and chemical properties of the deposited coatings also substantially depend on the laser energy density on the target and laser pulse duration. Thin-film coatings obtained by the femtosecond laser ablation of graphite have a more uniform surface and the amount of

ablated material droplets on it is less than in the case of ablation by nanosecond pulses producing a comparable energy density on the target [7, 8].

A different method for controlling the parameters of thin-film coatings, which is based on the use of the inverse flow of ablated particles scattered both by the particles of a plasma plume and gas molecules, was proposed in paper [9] and developed in [10]. This method was called the method of inverse laser deposition. It was shown in [9] that the morphology of films prepared by this method by irradiating a graphite target by nanosecond laser pulses in the nitrogen atmosphere was considerably better than the morphology of films obtained by the traditional method of direct deposition and its dependence on the laser radiation energy density and nitrogen pressure was weaker. At the same time, the preparation of thin-film carbon coatings by the method of inverse deposition with the use of femtosecond laser pulses was not considered in the literature. As a rule, such coatings are deposited by using crystalline or polycrystalline graphite targets. In this paper, we used a target made of a relatively new form of chemically pure graphite (99.99 %) – foam graphite with the density  $\rho = 0.7 \text{ g cm}^{-3}$ . The high efficiency of laser ablation of foam graphite due to its well developed absorbing surface was demonstrated in [11].

The aim of this paper is to perform a comparative study of the surface morphology of thin-film carbon coatings obtained by the methods of direct and inverse deposition in one experiment upon femtosecond laser ablation of foam graphite in the nitrogen atmosphere and also to determine the effective direct and inverse mass transfer of ablated particles.

## 2. Experimental

We used in experiments a 1.24- $\mu\text{m}$  femtosecond Cr:forsterite laser emitting 140-fs, 400- $\mu\text{J}$  pulses with a pulse repetition rate of 10 Hz [12].

Figure 1 presents the experimental scheme. Femtosecond laser radiation was focused by a lens with  $F = 10 \text{ cm}$  on a target at an angle of  $45^\circ$ . The laser beam spot size on the target surface was  $60 \times 80 \mu\text{m}$ . The laser energy density  $\varepsilon$  on the target achieved  $\sim 10 \text{ J cm}^{-2}$ , which corresponded to the laser radiation intensity on the target  $\sim 10^{14} \text{ W cm}^{-2}$ . The target was a narrow foam graphite foil strip of width 2000  $\mu\text{m}$  and thickness 160  $\mu\text{m}$  glued on a silicon [Si(100)] inverse-deposition collector. A Si(100) collector for the direct deposition of ablated particles was located at a distance of 1 cm from the target parallel to it, which did not block the incident laser radiation. No special machining of

V.M. Gordienko, V.A. D'yakov, I.A. Makarov, E.V. Rakov Department of Physics, M.V. Lomonosov Moscow State University, Vorob'evy gory, 119992 Moscow, Russia; e-mail: gord@femto.phys.msu.ru;

Yu.Ya. Kuzyakov Department of Chemistry, M.V. Lomonosov Moscow State University, Vorob'evy gory, 119992 Moscow, Russia;

M.A. Timofeev D.V. Skobel'tsyn Research Institute of Nuclear Physics, M.V. Lomonosov Moscow State University, Vorob'evy gory, 119992 Moscow, Russia

Received 5 July 2006; revision received 26 September 2006

Kvantovaya Elektronika 37 (3) 285–289 (2007)

Translated by M.N. Sapozhnikov

the surface of silicon collectors was performed. The target was fixed on a dual-axis computer-controlled translation stage. The whole target–collector system was placed into a vacuum chamber, which was evacuated for an hour with a roughing pump down to the residual pressure of no more than  $10^{-2}$  Torr and then, also for an hour, with a turbomolecular pump down to the residual pressure of no more than  $10^{-4}$  Torr. Then, nitrogen (99.5%) was admitted into the chamber up to a pressure of 0.3 Torr. This value corresponded to the pressure reported in the literature for which the direct and inverse deposition rates were approximately equal (upon irradiation by nanosecond laser pulses). The total number of laser shots during the film deposition was 72 000. The film surfaces were studied by using scanning electron and atomic-force microscopes, as well as by the method of X-ray photoelectron spectroscopy.

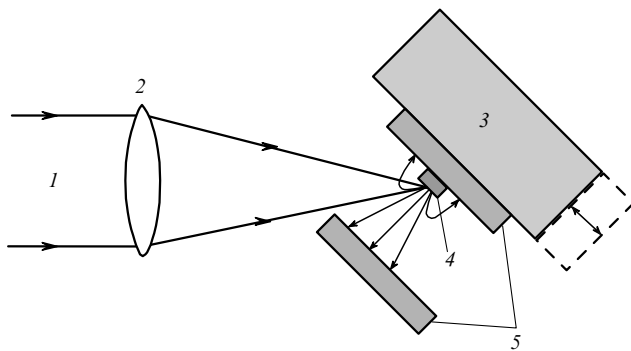


**Figure 1.** Experimental scheme: (1) radiation of a Cr : forsterite laser; (2) lens; (3) computer-controlled translation stage; (4) foam graphite target; (5) silicon collectors.

In addition, to estimate the volume of the target material ejected per laser shot upon irradiation of foam graphite by femtosecond pulses at a pulse repetition rate of 10 Hz, we performed additional experiments on the perforation of a 160- $\mu\text{m}$  thick foam graphite foil in the nitrogen atmosphere at a pressure of 1 Torr. The output signal of a photodetector based on a photodiode with an integrating sphere was fed via an analogue-to-digital converter to a digital oscilloscope and processed by using a special computer program. The instant of the foil puncture was determined by a drastic increase in the oscilloscope signal. The average number  $N$  of laser shots required for the target perforation under these conditions was  $250 \pm 50$ .

### 3. Results and discussion

Femtosecond laser pulses in our experiments were focused by a lens with the focal distance  $F = 10$  cm. The laser-beam diameter that we measured earlier by projecting its magnified image from the lens focus on a CCD camera was  $d = 10$   $\mu\text{m}$  (at the  $1/e$  intensity level). Therefore, the intensity of femtosecond laser radiation at the focus achieved  $\sim 3 \times 10^{15}$   $\text{W cm}^{-2}$ . Laser radiation was focused on the target visually by the maxima of the width of a plasma plume and ejection of macroparticles from the ablation region of foam graphite, which strongly depended on the deviation from the focus. The accuracy of focusing by this method (no more than 100  $\mu\text{m}$ ) proved to be sufficient, taking into account that the beam-waist length  $b$

estimated by the expression  $b = \pi d^2 / \lambda$  [13] was 260  $\mu\text{m}$  in experiments. Then, the focus was moved inside the target by 700  $\mu\text{m}$ , the laser-beam diameter being 60  $\mu\text{m}$  (at the  $1/e$  intensity level) and the laser radiation intensity on the target being  $\sim 10^{14}$   $\text{W cm}^{-2}$ . This method of focusing femtosecond laser radiation on the foam graphite target was used in all our experiments described here.

In experiments on the perforation of foam graphite foils by focused femtosecond laser pulses in the repetitively pulsed regime, a target was oriented at the angle of incidence of  $53^\circ$ . The effective thickness  $l_{\text{eff}}$  of the foil was 270  $\mu\text{m}$ . Because the number of laser shots required for the foil perforation was  $250 \pm 50$ , the average ablation depth  $l_a = l_{\text{eff}}/N$  per laser shot was  $1.1 \pm 0.2$   $\mu\text{m}$ . The crater size on the front surface of the target measured with an optical microscope was  $80 \times 60$   $\mu\text{m}$ , and therefore the total volume of the ablated material was  $V = \frac{1}{3}SH = 3 \times 10^{-7}$   $\text{cm}^3$ , where  $S$  is the area of the crater base on the surface target and  $H$  is the foam graphite foil thickness. Thus, the volume of the target material ejected per laser shot was  $V_1 = V/250 = (12 \pm 3) \times 10^{-10}$   $\text{cm}^3$ .

During femtosecond laser deposition, the target performed computer-controlled periodic horizontal displacements (at the average velocity 200  $\mu\text{m s}^{-1}$ ) along a band of length 0.4 cm. The stop time at the end points per passage was 2 s. After 30 successive passages over one horizontal band, the target was displaced vertically by 200  $\mu\text{m}$  to the next band. Upon repetitively pulsed irradiation of foam graphite foils on a silicon substrate by focused femtosecond laser pulses, the number of laser shots to one point within each band was 60–80 and 300 at the end points of the band. Thus, the base of the films in experiments on preparing thin-film coatings was carbon rather than the material of the substrate of the composite target. In addition, the finite ablation depth of the material within the band was 60–80  $\mu\text{m}$ , and therefore the laser irradiation intensity remained equal to  $\sim 10^{14}$   $\text{W cm}^{-2}$ .

Upon natural illumination, the interference pattern of a directly deposited film had the form of concentric colour rings, while this pattern for an inversely deposited film had the form of ellipses. We measured the distribution profiles of the deposited material as a function of the distance to the centre of the deposition region by using an atomic-force microscope. Preliminarily, marks were scratched on both films with a scalpel from the centre of the deposition region to its periphery. The width of each of the marks was  $\sim 100$   $\mu\text{m}$ . The scratch bottom represented a smooth surface with the roughness parameter (1 nm) coinciding with that measured for a probe silicon plate in the absence of a film. Thereafter we used an atomic-force microscope to measure the height of the corresponding ‘step’ in regions at the mark boundary preliminarily indicated under an optical microscope. As a result, we found that the diameter (at the  $1/2$  level) of the directly deposited film was 0.7 cm and its maximal thickness was 0.8  $\mu\text{m}$  (Fig. 2). The major and minor axes of the inversely deposited film were 0.7 and 0.9 cm, respectively (at the  $1/2$  level), and its maximal thickness was 0.6  $\mu\text{m}$ . The distribution of the material on the inverse-deposition collector was measured by the minor axes of the visible elliptic deposition rings, beginning from the edge of the foam graphite band (Fig. 2). The distribution of the material along the major axis of elliptic rings deposited on the inverse-deposition collector was estimated by assuming that the corresponding rings of the same colour

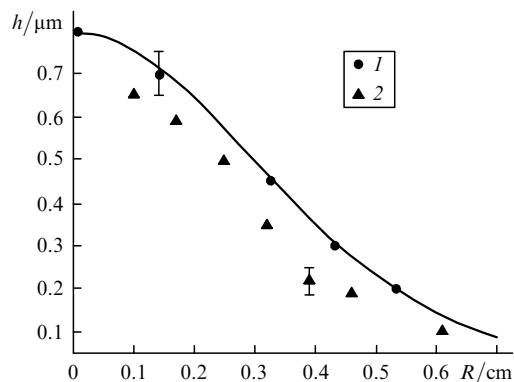


**Figure 2.** Dependences of the thickness  $h$  of directly (1) and inversely (2) deposited films on the radius  $R$ ; the solid curve is well described by the function  $\cos^n \theta$  ( $n = 11 \pm 1$ ), where  $\theta$  is the angle between the normal to the target surface and direction to the corresponding region on the direct-deposition collector.

preserve the thickness along the major and minor axes of the visible rings. Thus, the volumes  $V$  of the material deposited on the direct and inverse collectors of ablated particles proved to be almost identical and equal to  $3 \times 10^{-5} \text{ cm}^3$  (correspondingly, the volume deposited per laser shot to each of the sides was  $V_1 = V/72000 = 4 \times 10^{-10} \text{ cm}^3$ ). As a result, the total volume of the ablated material deposited on the direct and inverse-deposition collectors was  $\sim 70\%$  of the total volume of the ablated material.

The scotch-test of both of the films showed that films could not be removed with the help of a paint scotch having a relatively weak cohesion with the film surface. However, when an office scotch was used, the central regions of the

films could be readily removed but their periphery remained on the silicon substrate.

The chemical composition of the films studied by the method of X-ray photoelectron spectroscopy was as follows: C (88%), O (12%) (directly deposited film) and C (90%) and O (10%) (inversely deposited film). No nitrogen was found in the deposited films.

The surface of the directly and inversely deposited films was studied with a LEO-1430VP electron microscope near central regions and at a distance of 0.4 cm from them. The electron-microscope photographs of films of size  $80 \times 100 \mu\text{m}$  (Fig. 3) demonstrate that the central surface regions of the directly deposited film contain large particles of size  $\sim 1 \mu\text{m}$  and more (Fig. 3). Their number and size decrease at the periphery of the deposition region. At the same time, the inversely deposited film virtually does not contain microparticles in its central region, while its surface at the periphery appears as the surface of the smooth target. The surface structures of directly and inversely deposited films outside microparticles were studied by photographs obtained with a large magnification ( $6 \times 8 \mu\text{m}$ ). The directly deposited film has a more porous, large-dispersion structure, both in the central region and at the periphery, compared to the surface structure of the inversely deposited film. Note also that the central surface of the directly deposited film consists of spherical conglomerates, while at the periphery these conglomerates have an arbitrary shape. This fact can indicate to the nonuniform radial distribution of the chemical composition of deposited particles in the directly deposited film. The structure of the inverse deposition film exhibits a weak radial dependence of the shape of deposited particles.

We studied the morphology of the regions (of size  $10 \times 10 \mu\text{m}$ ) of directly and inversely deposited films by

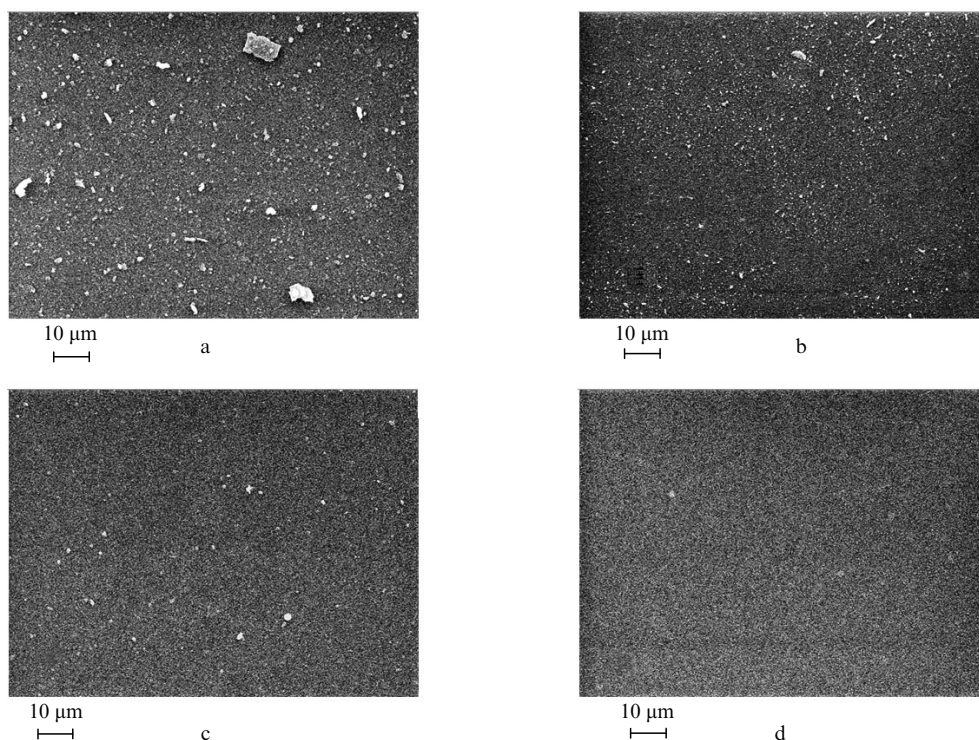


**Figure 3.** Photographs of the surfaces of directly (a, b) and inversely (c, d) deposited films obtained with a LEO-1430VP scanning electron microscope; (a, c) central deposition regions; (b, d) peripheral regions (0.4 cm from the centre).

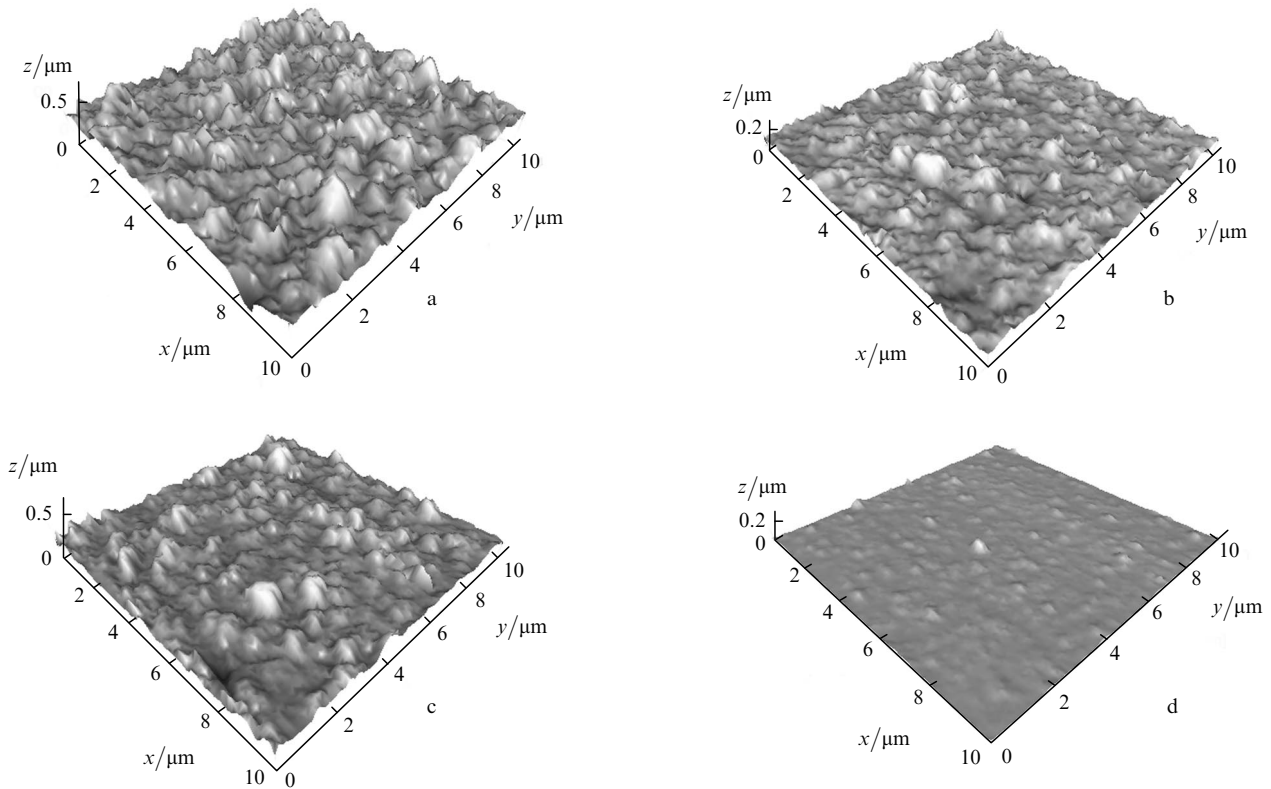


**Figure 4.** Photographs of the surfaces of directly (a, b) and inversely (c, d) deposited films obtained with a SBM Stand Alone Smena scanning probe microscope; (a, c) central deposition regions; (b, d) peripheral regions (0.4 cm from the centre).

using an atomic-force microscope and determined the surface roughness parameter  $dh$  equal to the deviation of the film thickness from its average value in the specified area of the corresponding region of the film surface (Fig. 4). Our measurements showed that the roughness parameter changed depending on the radius from  $0.055 \mu\text{m}$  ( $0.04 \mu\text{m}$ ) at the film centre to  $0.02 \mu\text{m}$  ( $0.01 \mu\text{m}$ ) at a distance of 0.4 cm from the centre for directly (inversely) deposited films, respectively (Fig. 5).

Thus, we have found that the surface of inversely deposited films almost does not contain droplets of the

ablated material and the surface structure is denser and more uniform than that of the directly deposited film (the surface roughness parameter is lower). The high quality of the surface of the inversely deposited carbon film is apparently explained by the fact that massive and high-energy particles of the ablated material escape forward and do not backscatter in the interaction with a buffer gas.

#### 4. Conclusions

We have performed for the first time a comparative study of the direct and inverse femtosecond laser deposition of carbon films in the nitrogen atmosphere.

It has been found that the surface of the inversely deposited film almost does not contain microparticles, unlike the surface of the directly deposited film covered by numerous microparticles. The dependence of the surface roughness parameter of films on the radius was measured. It is shown that the surface of the inversely deposited film is smoother than that of the directly deposited film. The ablation rates of foam graphite and the volumes of the material ejected and deposited per laser shot were measured.

However, the question of the influence of the energy density of ablating femtosecond laser pulses on a target and the pressure of a buffer gas on the surface morphology of inversely deposited thin-film coatings remains open.

**Acknowledgements.** This work was supported by the Russian Foundation for Basic Research (Grant Nos 04-03-32864 and 05-02-16476).

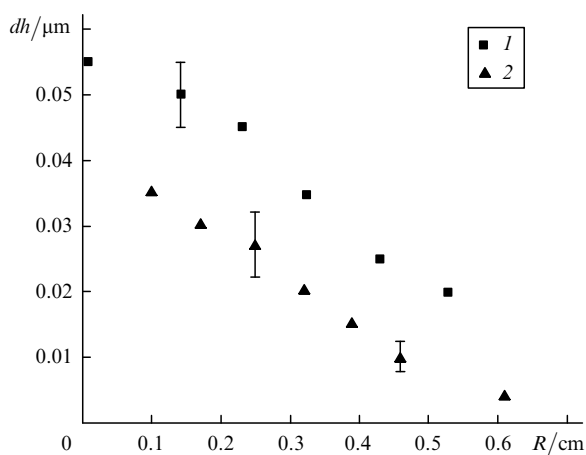


**Figure 5.** Dependences of the surface roughness parameter  $dh$  for directly (1) and inversely (2) deposited films on the radius  $R$ .

## References

1. Geretovszky Z., Kantor Z., Bertoti I., Szörenyi T. *Appl. Phys. A*, **70**, 9 (2000).
2. Roy S., Papakonstantinou P., Mccann R., Mclaughlin J., Klini A., Papadogiannis N. *Appl. Phys. A*, **79**, 1009 (2004).
3. Katsuno T., Godet C., Orianges J.C., Loir A.S., Garrelie F., Catherinot A. *Appl. Phys. A*, **81**, 471 (2005).
4. Gareth M.F., Ashfold M.N.R., Henley S.J. *J. Appl. Phys.*, **99**, 014309-1 (2006).
5. Henley S.J., Carey J.D., Silva S.R.P., Fuge G.M., Ashfold M.N.R., Anglos D. *Phys. Rev. B*, **72**, 205413-1 (2005).
6. Willmott P.R., Huber J.R. *Rev. Mod. Phys.*, **72**, 315 (2000).
7. Szörenyi T., Fogarassy E., Fuchs C., Hommet J., Le Normand F. *Appl. Phys. A*, **69**, 941 (1999).
8. Acquaviva S., Perrone A., Zocco A., Klini A., Fotakis C. *Appl. Surf. Sci.*, **373**, 266 (2000).
9. Szörenyi T., Hopp B., Geretovszky Z. *Appl. Phys. A*, **79**, 1207 (2004).
10. Egerhazi L., Geretovszky Zs., Szorenyi T. *Appl. Surf. Sci.*, **247**, 182 (2005).
11. Kudryashov S.I., Karabutov A.A., Zorov N.B., Kuznetsov S.V., Kuzyakov Yu.Ya. *Proc. SPIE Int. Soc. Opt. Eng.*, **2801**, 240 (1999).
12. Gordienko V.M., Ivanov A.A., Podshivalov A.A., Savelev A.B., Rakov E.V. *Laser Phys.*, **16**, 1 (2006).
13. Akhmanov S.A., Nikitin S.Yu. *Fizicheskaya optika* (Physical Optics) (Moscow: Nauka, 2004).